Numerical Investigation of the Temperature Distribution in PCM-integrated Solar Modules

Matti Grabo, Daniel Weber, Andreas Paul, Tobias Klaus, Wolfgang Bermpohl, Stefan Krauter, Eugeny Y. Kenig*

Paderborn University, Pohlweg 55, D-33098 Paderborn, Germany
eugeny.kenig@upb.de

Both lifetime and efficiency of photovoltaic (PV) modules are negatively affected by high and/or strongly fluctuating temperatures. An approach to improve the thermal performance is to add a phase change material (PCM) to the layer composition of PV modules. In order to be able to determine design parameters of the PCM, e.g. layer thickness of the PCM, melting point or chemical composition, a mathematical 1D-model describing the transient temperature distribution across the module was developed. It considers all relevant heat transfer mechanisms – conduction, convection and radiation – as well as the melting-solidification processes of the PCM. The model is solved numerically by an iterative, implicit algorithm implemented in MATLAB. Input factors include geometrical parameters and material properties as well as time-dependent weather effects (irradiance, ambient temperature, wind speed and direction). To determine these factors, either locally measured data or values derived by empirical models from literature can be employed. The simulated temperature distribution was validated against measured temperatures with an average deviation of ±1.7 K and used as an input for a module lifetime model. The latter model showed that the integration of a PCM into the layer composition could increase the lifetime of a PV module by up to 10 y, yet at the cost of a lower energy generation which is reduced by about 12 % compared to PV modules without PCM.

1. Introduction

The International Energy Agency (IEA) predicts a growth of installed photovoltaic (PV) capacity from 398 GW in 2017 to about 1,100 GW in the year 2023 (International Energy Agency, 2018). Increasing the efficiency and lifetime of solar modules are two of the keystones for realizing this scenario. For both these characteristics, the operating temperature inside a module represents a crucial factor: stable, high temperatures lead to a low electrical output, whereas high temperature fluctuations caused by temporary shading or wind induce mechanical stresses and hence lead to degradation in the solar module. An approach to reduce the operating temperature and to smoothen its fluctuation is to integrate a phase change material (PCM) into the layer structure of PV modules. Huang et al. (2004) were among the firsts to investigate the impact of PCMs attached to PV modules by experiments and finite-volume simulations for building integrated PV modules. They were able to maintain a temperature lower than 36.4°C for 80 min with their set-up. This was achieved by employing a PCM layer of 20 mm and aluminium fins. The fins were required to enable an even heat distribution within the PCM, because common PCMs generally have a low thermal conductivity (Liu, 2018). To address the problem of low conductivity, a more recent experimental study by Japs et al. (2013) compared conventional PCMs with PCMs having enhanced thermal conductivity due to an additional compound. However, since the mass fraction of the actual PCM in a compound mixture is reduced, the overall heat capacity decreases, which weakens the cooling effect. On the modelling side, Biwole et al. (2013) aimed to improve the model suggested by Huang et al. (2004) by implementing their test case into a finite-elements model with a modified buoyancy term in the momentum equations. Lo Brano et al. (2014) developed a thermal model of a PV module coupled with a PCM storage based on an explicit finite-difference method, which showed a mean average error of around ±6 K compared to field measurements. Since their explicit finite-difference scheme requires a stability criterion, the authors excluded the actual silicon cell with its high thermal conductivity in order to allow for a larger time step,

which resulted in a loss of accuracy. More recent studies use an approach based on the admixture of nanoparticles to the PCM to increase the module efficiency. For instance, using Al₂O₃ nanoparticles, Nada et al. (2018) were able to increase the efficiency by up to 12 %. Regarding the PV/PCM module thermal modelling, a very detailed finite element model was proposed by Nouira and Sammouda (2018), who investigated the performance of a PV/PCM module under varying conditions; in particular, the effect of dust layer thickness is worthy of mentioning. The authors found that dust can cause up to 3 W decrease of PV capacity. Another recent work published by Arici et al. (2018) studied the economical optimization of PV/PCM-systems with a simplified numerical model based on explicit finite-differences incorporating the actual solar cell. This model was validated against the data from Lo Brano et al. (2014) with a ±2 K deviation and used to compare different PCMs for different Mediterranean locations in different times of the year. They found that the optimal PCM layer thickness varies with the course of the year and that using PCMs for the regulation of the cell temperature is only feasible, if a significant decrease of investment cost for PCMs is reached. An aspect briefly addressed in their paper as well as in other publications is the expected positive effect of PCMs on the PV module lifetime. However, no detailed explanation was found in literature, which degradation mechanisms within the module are affected by the integration of PCMs and how this positive effect for the lifetime can be quantified.

The aim of the present work was to describe and quantify the aforementioned degradation mechanisms, both without and with PCM. Accordingly, a new coupled thermal degradation model was developed. Since degradation is enhanced by thermal fluctuations, a good understanding of the actual heat transfer processes within both regular and PCM-integrated solar modules is required. First, a thermal model was developed and implemented into MATLAB based on the implicit finite-differences method, allowing for a good resolution of the individual layers of PV modules and especially of the solar cell. The resulting cell temperature profiles were then used to estimate the damage caused by temperature fluctuations using the Coffin-Manson model.

2. Mathematical modelling

2.1 Thermal model

PCM-integrated PV modules consist of multiple material layers with different thermal properties illustrated in Figure 1. The module is exposed to ambient impacts, such as solar irradiance, convection and thermal radiation. Convection is caused either by wind, or by free convection, or by a combination of both, whereas thermal radiation results from the radiative heat exchange between the module and the sky and/or the ground. Heat conduction takes place within and between the module layers and can lead to a phase change of the PCM.
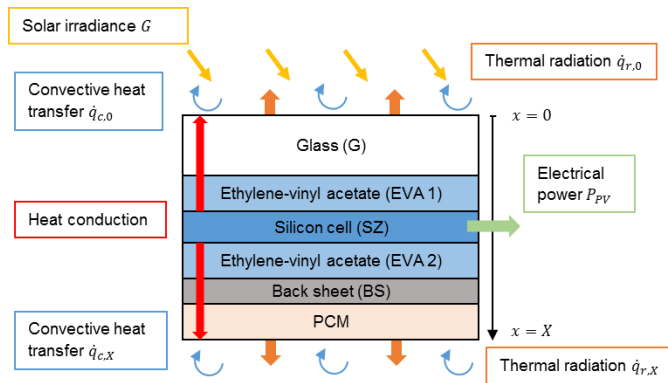

Figure 1: Schematic of a solar module layer structure with ambient impacts and heat transport processes

Assuming that heat losses through the module frame can be neglected and the ratio of the surface area to the module thickness is relatively small (i. e. assuming a one-dimensional domain), the following governing equation describing the heat transport processes within the PCM-integrated module can be obtained:

$$\rho c_p \frac{\partial T(x,t)}{\partial t} = \frac{\partial}{\partial x}\left(\lambda \frac{\partial T(x,t)}{\partial x}\right) + Q(x,t) \tag{1}$$

with temperature T, time t, thermal conductivity λ, density ρ and heat capacity c_p.

The source term $Q(x,t)$ is used to govern the heat generation within the first three layers of thickness X by solar irradiance G, absorbance δ and transmittance τ as well as the phase change within the PCM:

$$Q(x_G, t) = \delta_G \cdot \frac{G}{X_G} \tag{2}$$

$$Q(x_{EVA1}, t) = \delta_{EVA1} \cdot \tau_G \cdot \frac{G}{X_{EVA1}} \tag{3}$$

$$Q(x_{SZ}, t) = \tau_{EVA} \cdot \tau_G \cdot \frac{G}{X_{SZ}} - \frac{P_{PV}(T)}{A_{SZ} X_{SZ}} \tag{4}$$

The electrical power output $P_{PV} = \eta_{PV} \cdot G \cdot A_{SZ}$ from the surface of the solar cells A_{SZ} was determined by using the correlation of Evans and Florschuetz (1977) for the efficiency η_{PV}, which is convenient, because it only relies on the cell temperature and module parameters given by the manufacturer, such as reference efficiency η_{Ref}, temperature coefficient β_{Ref} and reference temperature T_{Ref}:

$$\eta_{PV} = \eta_{Ref}\left[1 - \beta_{Ref}\left(T_{SZ} - T_{Ref}\right)\right] \tag{5}$$

For PCM-integrated modules, the phase change front within the PCM has to be effectively captured via the evolution of latent heat. A common approach is to include the latent heat evolution as a source term as follows:

$$Q(x_{PCM}, t) = -\rho L \frac{\partial \gamma}{\partial t} \tag{6}$$

The actual liquid fraction γ is zero, when the PCM is in a solid state, one, when it is in a liquid state, and between zero and one, when its temperature lies between the solidus and liquidus temperatures. A more detailed description of the melting/solidification modelling is given in (Voller and Swaminathan, 1991).

The following boundary conditions were applied at the top and the bottom sides of the module:

$$\lambda \frac{\partial T}{\partial x}\Big|_{x=0} = \dot{q}_{r,0} + \dot{q}_{c,0} \tag{7}$$

$$-\lambda \frac{\partial T}{\partial x}\Big|_{x=X} = \dot{q}_{r,X} + \dot{q}_{c,X} \tag{8}$$

As initial condition, the temperature field was set equal to the ambient temperature T_∞, which was retrieved from measurements (see Section 3).

The radiative heat flux $\dot{q}_r$ resulting from radiative heat exchange of the top and bottom sides of the module with the sky and ground, correspondingly, was calculated using a radiative heat transfer coefficient h_r, which was determined according to the Stefan-Boltzmann law. This enables the radiative heat flux, Eq(9), to be implemented similarly to the convective heat flux $\dot{q}_c$, Eq(10):

$$\dot{q}_{r,0/X} = h_{r,0/X}\left(T_{0,X} - T_{sky/ground}\right) \tag{9}$$

$$\dot{q}_{c,0/X} = h_{c,0/X}\left(T_{0,X} - T_\infty\right) \tag{10}$$

The temperature of the ground T_{ground} was set equal to the ambient temperature. In order to estimate the temperature of the sky T_{sky}, four different correlations were applied, while the convective heat transfer coefficient h_c was estimated with five different correlations. This gave altogether 20 possible combinations to determine the boundary conditions.

2.2 Degradation model

The temperature distribution calculated by the thermal model was used as input for a degradation model to estimate failure induced by thermal cycling. The fatigue and the resulting degradation can be determined with a model described by Weber et al. (2018), which is briefly outlined below.

First, the temperature cycles during the operational period had to be detected. Therefore, the rain flow counting algorithm was used, which detects the relevant full and half cycles in a fluctuating load quantity. Its output – applied to the calculated temperature cycle of the module – is the amplitude of the temperature cycle ΔT, the duration time t_d of a half cycle and the maximum and mean temperature (T_{max} and $\bar{T}$, respectively). These thermal cycles cause mechanical stresses in the different layers of the solar module due to different coefficients of thermal expansion. The stresses can lead to degradation and eventually to failure. As discussed in (Weber et al., 2018), failure is caused, amongst others, by mechanical breakage of the interconnector between the cells. In order to estimate the effect of mechanical stresses on the module lifetime, the Coffin-Manson model (Coffin,

1954) was used, which describes the number of cycles until failure N_f as a function of the mechanical stress amplitude:

$$N_\mathrm{f} = K\Delta T^{-2} f^{\frac{1}{3}} e^{\frac{E_a}{\sigma_\mathrm{B} T_\mathrm{max}}} \tag{11}$$

(11) determines N_f for one thermal cycle characterized by the temperature amplitude ΔT, the cycle frequency f, the material-dependent activation energy E_a and the maximum cycle temperature T_max. Here, σ_B denotes the Boltzmann constant. The activation energy $E_\mathrm{a} = 0.5$ eV was chosen according to the strain range of copper. The parameter K has to be adjusted via measurements or finite element analysis, however it is not required for a relative comparison between modules with and without PCM. To evaluate the damage D for a given N_f, the Palmgren-Miner hypothesis was used:

$$D = \sum_i \frac{1}{2N_{f,i}} \tag{12}$$

The end of life is reached when the damage D equals one.

3. Experimental

In order to validate the thermal model, experiments were performed in the PV laboratory on the roof of Paderborn University shown in Figure 2 (left). The experimental set-up consists of two photovoltaic modules PX230 by the manufacturer Sunset Solar GmbH with a nominal capacity of 230 W, a reference efficiency of $\eta_{Ref} = 14.3$ %, a temperature coefficient of $\beta_{Ref} = 0.325 \frac{\%}{K}$ and a reference temperature of $T_{Ref} = 25\,°C$. One of such modules was used as a reference, whereas a PCM was attached to the other one. On the backside of the modules PT100 elements were attached at the locations indicated in Figure 2 (right). Subsequently, the PCM layer was added in such a way that the sensors are positioned between the back sheet and the PCM. The modules inclination to the surface was 30 °. Measured data include module temperatures, wind speed and direction, ambient temperature and solar irradiance.
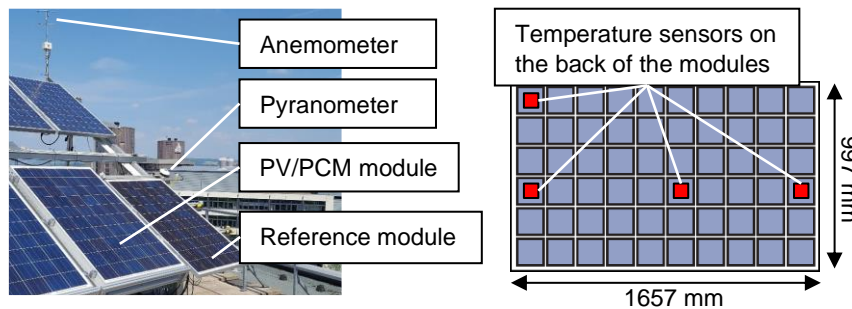

Figure 2: Experimental set-up on the roof of Paderborn University (left) and locations of PT100 elements on the modules (right)

The PCM is a copolymer compound consisting of paraffin and graphite, which helps to increase the heat conductivity as shown in (Sonnenrein et al., 2015). The resulting latent heat was assumed to be 160 kJ/kg over the melting interval from the solidus temperature of 40 °C to the liquidus temperature of 43 °C. The thermal properties of the individual layers of the module are listed in Table 1.

Table 1: Thermal properties of the individual layers of the considered PV module

Layer	Thickness s [mm]	Heat conductivity k [W/m K]	Heat capacity c_p [J/kg K]	Density ρ [kg/m³]
Glass	4	1.8	500	3000
EVA1	0.45	0.35	2090	960
Solar cell (polycrystalline)	0.2	148	677	2330
EVA2	0.45	0.35	2090	960
Back sheet (polyamide)	0.35	0.2	1700	1140
PCM (paraffin)	3		1800	
Liquid		0.6		760
Solid		1		880

The measured temperatures are illustrated in Figure 3 (left) for the day June 20th, 2018. As can be seen, the temperature of the PCM-module shows lower fluctuations, but it is generally higher. This is especially the case in the afternoon, when the PCM has already melted and only acts as thermal insulator on the backside of the module. Regarding the generated electrical energy, due to the higher temperatures, the PCM-module produces approximately 12 % less energy than the reference module, as shown in Figure 3 (right).
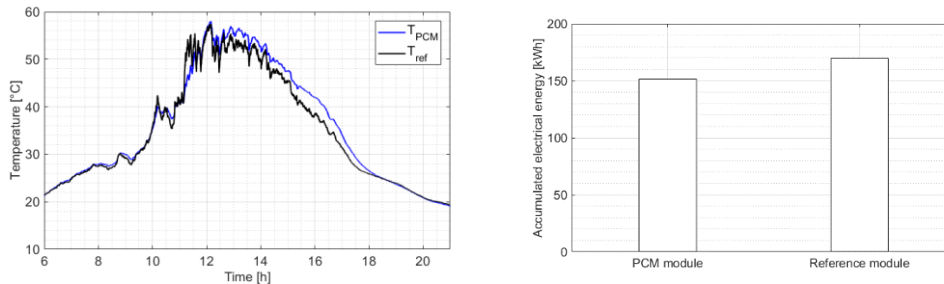

Figure 3: Comparison of temperatures on June 20th, 2018 for the PCM and the reference module (left) and comparison of generated electrical energy for the second half year of 2018 (right)

4. Simulations and results

Simulations were performed for four days with different weather conditions in summer 2018: a sunny day with occasional cloudiness (June 20th), a sunny day with no clouds (July 1st), a cloudy day (August 20th) and a day with fluctuating cloudiness (August 25th). First, the different correlations for the temperature of the sky and the heat transfer coefficient were applied, while simulations were performed for all four days. The parameter combination giving the least average deviation (±1.7 K) from the measured data for all considered days was found to be: $T_{sky} = T_\infty - 6$ for the temperature of the sky given by Whillier (1967) and $\alpha_c = 5.74 \cdot v_f^{0.8} \cdot L^{-0.2}$ for the convective heat transfer coefficient suggested by Sartori (2006), with the module length L and the free wind speed v_f. From the resulting temperature profiles, the accumulated damage was calculated and normalized to the maximum damage taken by the reference module on the day with the highest temperature fluctuations (June 20th) $D_{ref,max}$. A comparison of the accumulated damages for June 20th and the relative accumulated damage taken by the PCM-module D_{PCM} on the considered days are shown in Figure 4.
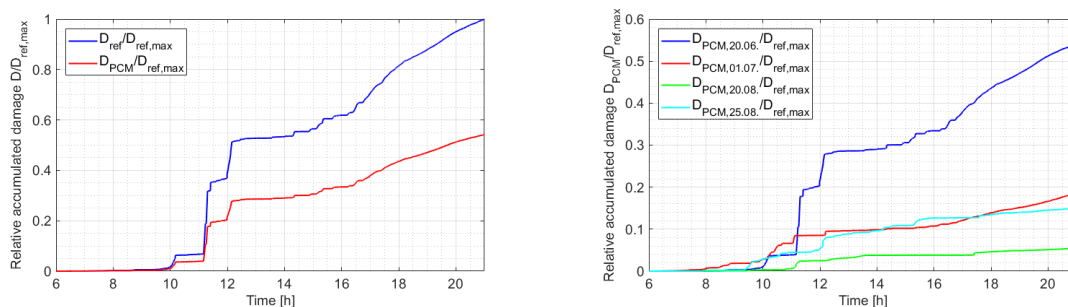

Figure 4: Relative accumulated damage for June 20th – the day with the highest temperature fluctuations (left) and relative accumulated damage of the PCM-module for the four considered days (right)

As can be seen in Figure 4a, the relative accumulated damage on June 20th was around 45 % lower for the PCM-module compared to the reference module; this was similar for the other days considered. Assuming that these four days are representative for typical daily temperature profiles throughout a year, the lifetime of the PV module interconnector could be increased from actual 25 y to over 35 y. Another finding illustrated in Figure 4b is that the damage on June 20th is more than doubled the damage on July 1st, which indicates that stable, high temperatures are less harmful for the module lifetime than strong temperature fluctuations.

5. Conclusions

In this paper, a simple, coupled thermal degradation model for PCM-integrated PV modules was suggested. First, the thermal model was established based on the consideration of different heat transport processes, such

as heat conduction, convection, thermal radiation and the phase change of the PCM. The mathematical model was discretized using an implicit finite-difference method, and the results were compared with field-measured data. The resulting mean average error over four representative days in summer 2018 fell within ±1.7 K, hence the thermal model can be considered valid. Due to the fact, that no stability criterion is required for implicit methods, larger time steps could be used which made it possible to model the thermally well conducting solar cell. The cell temperature is required to determine the power generation by the module; furthermore, it serves as input in the degradation model. Degradation was calculated using the algorithm described in the previous paper (Weber et al., 2018). The estimated accumulated damage for four different days in 2018 of the PCM-module was approximately 45 % lower than for the reference module resulting in an increase of lifetime by over 10 y. However, the PCM integration resulted in a 12 % reduction of generated electrical power compared to a reference module without PCM. Consequently, an economic study has to be performed to investigate whether the lower energy output combined with a higher investment cost for the PCM outweigh the actual gain in lifetime. Furthermore, in order to validate the degradation model accelerated stress tests will be performed.

Acknowledgments

References

Arici M., Bilgin F., Nizetic S., Papadopoulos A. M., 2018, Phase change material based cooling of photovoltaic panel: A simplified numerical model for the optimization of the phase change material layer and general economic evaluation, Journal of Cleaner Production, 189, 738-745.

Biwole P. H., Eclache P., Kuznik F., 2013, Phase-change materials to improve solar panel's performance, Energy and Buildings, 62, 59-67.

Coffin L. F., 1954, A study of the effects of cyclic thermal stresses on a ductile metal, Transactions of the ASME, 76, 931-950.

Evans D. L., Florschuetz L. W., 1977, Cost studies on terrestrial photovoltaic power systems with sunlight concentration, Solar Energy, 19, 255-262.

Huang M. J., Eames P. C., Norton B., 2004, Thermal regulation of building-integrated photovoltaics using phase change materials, International Journal of Heat and Mass Transfer, 47, 2715-2733.

International Energy Agency, 2019, Solar energy <iea.org/topics/renewables/solar> accessed 29.04.2019.

Japs E., Sonnenrein G., Steube J., Vrabec J., Kenig E. Y., Krauter S., 2013, Technical Investigation of a photovoltaic module with integrated improved phase change material, 28th European Photovoltaic Solar Energy Conference and Exhibition, 500-502.

Liu X., 2018, Study on the temperature characteristics of phase-change energy storage building materials based on ANSYS, Chemical Engineering Transactions, 66, 385-390.

Lo Brano V., Ciulla G., Piacentino A., Cardona F., 2014, Finite difference thermal model of a latent heat storage system coupled with a photovoltaic device: Description and experimental validation, Renewable Energy, 68, 181-193.

Nouira M., Sammouda H., Numerical study of an inclined photovoltaic system coupled with phase change material under various operating conditions, Applied Thermal Engineering, 141, 958-975.

Nada S.A., El-Nagar D.H., Hussein H.M.S., 2018, Improving the thermal regulation and efficiency enhancement of PCM-Integrated PV modules using nano particles, Energy Conversion and Management, 166, 735-743

Sartori E., 2006, Convection coefficient equations for forced air flow over flat surfaces, Solar Energy, 80, 1063-1071.

Sonnenrein G., Elsner A., Baumhögger E., Morbach A., Fieback K., Vrabec J., 2015, Reducing the power consumption of household refrigerators through the integration of latent heat storage elements in wire-and-tube condensers, International Journal of Refrigeration, 51, 154-160.

Voller V. R., Swaminathan C. R., 1991, General source-based method for solidifcation phase change, Numerical Heat Transfer, Part B Fundamentals, 19(2), 175-189.

Weber D., Jani M., Grabo M., Wallscheid O., Böcker J., Klaus T., Krauter S., 2018, Lifetime Extension of Photovoltaic Modules by Influencing the Module Temperature Using Phase Change Material, 7th World Conference on Photovoltaic Energy Conversion, Waikoloa, USA, 784-789.

Whillier A., 1967, Design factors influencing solar collectors in low temperature engineering applications of solar energy, ASHRAE, New York, USA. objWordDoc